A Robust Background Initialization Algorithm with Superpixel Motion Detection

Zhe Xu, Biao Min, Ray C. C. Cheung*

Department of Electronic Engineering, City University of Hong Kong, Hong Kong, China

Abstract

Scene background initialization allows the recovery of a clear image without foreground objects from a video sequence, which is generally the first step in many computer vision and video processing applications. The process may be strongly affected by some challenges such as illumination changes, foreground cluttering, intermittent movement, etc. In this paper, a robust background initialization approach based on superpixel motion detection is proposed. Both spatial and temporal characteristics of frames are adopted to effectively eliminate foreground objects. A subsequence with stable illumination condition is first selected for background estimation. Images are segmented into superpixels to preserve spatial texture information and foreground objects are eliminated by superpixel motion filtering process. A low-complexity density-based clustering is then performed to generate reliable background candidates for final background determination. The approach has been evaluated on SBMnet dataset and it achieves a performance superior or comparable to other state-of-the-art works with faster processing speed. Moreover, in those complex and dynamic categories, the algorithm produces the best results showing the robustness against very challenging scenarios.

Keywords: Background initialization; superpixel; motion detection; density-based clustering

1. Introduction

Scene background initialization refers to approaches automatically producing a stationary scene without foreground objects, given a set of training frames. It is a critical step in many computer vision and video processing applications such as object detection and tracking [1, 2], video segmentation [3], video coding [4, 5, 6], video inpainting [7] and so on. In such applications, obtaining the background image is generally a pre-processing step and the clear background can make the processing more effective.

---

*Corresponding author

Email addresses: zhexu22-c@my.cityu.edu.hk (Zhe Xu),
biaomin3-c@my.cityu.edu.hk (Biao Min), r.cheung@cityu.edu.hk (Ray C. C. Cheung)
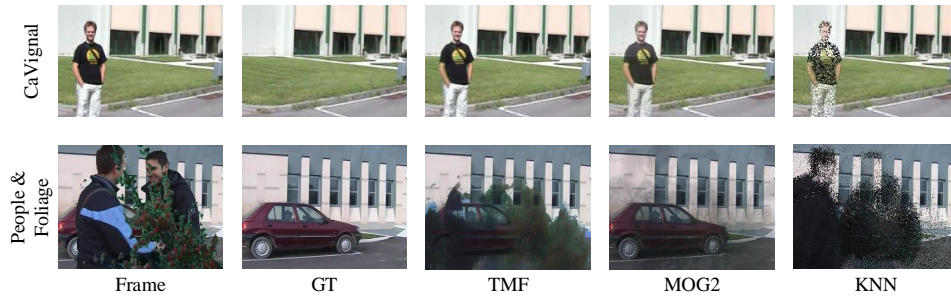
Fig. 1: Failing background initialization examples. (The first column is one representative frame in original sequence, the second column is the true background image and the rest columns are backgrounds obtained by TMF, MOG2 and KNN, respectively.)

Several simple background initialization approaches directly choose one frame from sequence as the background with the assumption that the frame is free of foreground objects [8]. However this assumption is not feasible in many video surveillance situations. For example, in crowded shopping malls, there may exist moving people in every frame so the extracted background is not accurate. Another simple and intuitive approach is to adopt a temporal median filter (TMF) for background initialization [8]. TMF can tolerate moving object noise as long as foreground objects at any position take less than half of the estimation period. In addition, the computer vision library OpenCV[1] provides two prevalent background modeling methods. One is based on adaptive Gaussian mixture model called MOG2 [9] and another is based on k-nearest neighbors (KNN) [10].

Although the above-mentioned three methods can produce satisfied results for simple situations, in complex scenarios with heavy foreground cluttering or long-time stationary objects, most of them cannot eliminate all foreground components effectively which leads to image blurring. Fig. 1 demonstrates two failing background initialization examples. *CaVignal* shows a situation called intermittent motion, in which the man stands still in the left of the scene for a long time. All three methods wrongly include the man in the final estimated background. While in *People & Foliage*, large portion of the scene area is occupied by leaves and men. This wide clutter leads to image blurring especially for TMF and KNN. As a result, a robust background initialization algorithm is demanded for complex scenes.

In general, the performance of background initialization is affected by following several factors. Firstly, illumination changes (such as outdoor sunlight change or indoor lights switching on) may cause illumination variance in different regions in the estimated background. Secondly, the background in certain regions may only be visible for a short time so foreground objects are wrongly included in the result. This occurs when there exists a clutter of moving foregrounds occupying large portion of the scene area or there exists stationary foreground object in the estimation period (i.e., intermit-

---

[1]https://opencv.org

2

tent motion). Thirdly, some motion objects may not be considered as the foreground, including global motion caused by camera jitter and moving background like fountain or waving trees.

In this paper, a robust background initialization algorithm based on superpixel motion detection with relatively low computational complexity is proposed. Both spatial and temporal characteristics of frames are adopted to effectively eliminate foreground objects. An illumination change detection using histogram equalization is firstly performed and a subset of sequence with consistent illumination condition is selected for further processing. Then, simple linear iterative clustering (SLIC) superpixel algorithm [11] is employed to segment images to preserve spatial correlations and temporal difference motion detection is performed in superpixel level to extract motionless regions, which is called superpixel motion detection (SPMD). A low-complexity density-based clustering generates reliable background candidates for each pixel and the final result is selected from candidates with both the first and last frame as the reference. The motion detection is a superpixel-level strategy while the density-based clustering is pixel-level. Thus the whole algorithm is a hybrid method. To extract a clear background in complex scene, some new approaches are adopted including:

1. An illumination change detection scheme is adopted to alleviate illumination variance in the final result. Thus for sequences with various illumination conditions, the algorithm can produce stable background image. Section 3.2 will detail this illumination change detection method.

2. The superpixel based segmentation is performed to preserve image texture information, thus SPMD considers both spatial and temporal correlation. Compared with normal pixel-wise motion detection, it can remove relevant moving pixels more effectively. The SPMD method is presented in Section 3.3.

The results show that our algorithm can effectively and robustly estimate an accurate background on SBMnet dataset, which is comparable or superior to other state-of-the-art works. In addition, the computational complexity is low making it at least twice faster than other comparable algorithms. The rest of this paper is organized as follows. Section 2 reviews previous related approaches. The proposed robust background initialization algorithm is introduced in detail in Section 3. Experimental results are provided in Section 4. At last, Section 5 gives the conclusion.

2. Related Work

As a basic step in computer vision and video processing application, background initialization problem has been extensively studied and corresponding approaches have been proposed. In this section, some related background initialization approaches are briefly discussed.

A simple scheme to extract a background is the temporally statistical approach. In [12], Lai *et al.* use a running mode and running average algorithms to initialize the stationary background. A scoreboard is used to keep the pixel variations. For pixels with large variations, the running mode algorithm is selected. Otherwise the running average method is used for lower complexity. In [13], an iterative approach using median blending and spatial segmentation is proposed. In each iteration, moving objects

are detected based on motion compensation and removed for background initialization. The median value of the remaining parts is taken as the background. In [14], a two-step framework is proposed for background initialization. All stable subsequences are firstly identified based on a frame difference method. Then the most reliable subsequence is determined and the mean value of selected subsequence is taken as the background value. In [15], Stauffer *et al.* propose a background initialization method by modeling each pixel as a Gaussian Mixture Model (GMM). Each pixel is classified as background or foreground based on whether the pixel value fits the current background distribution. In [9], Zivkovic proposes a similar GMM method for background initialization. The number of components for each pixel is updated in an online process, thus the algorithm can automatically adapt to the scene. In [16], a background subtraction algorithm is firstly performed to reduce the set of value candidates for each pixel. This candidates selection is performed on a patch. Then for each pixel, the temporal median filter for the candidates is applied to generate a stable background.

To avoid parameter tuning problem, some methods use a nonparametric scheme to initialize the background image. Liu *et al.* [17] present a background initialization method based on nonparametric model. The most reliable background mode is calculated based on mean shift clustering and the value is taken as the estimated background. Elgammal *et al.* [18] introduce a nonparametric background modeling by estimating the probability of pixel intensity values based on kernel estimator. The pixel is then considered whether to be a background based on estimated probability. In [19], Zhang *et al.* propose a two-stage background initialization method. The first stage monitors pixel intensity to identify background variations and creates a look-up table as the intensity distribution. Then in the second stage, based on whether current pixel is in the look-up table, the final background is determined.

In recent years, new approaches have been proposed to generate clear background images in complex scenes. These algorithms adopt some new techniques such as matrix or tensor completion, neural networks and so on. In [20], the background estimation is modeled as a matrix or tensor completion task. The redundant frames are eliminated first and moving regions are represented by zeros. Then various matrix or tensor completion methods are utilized to reconstruct the whole frame sequence with moving objects removed. The background image is finally initialized as the mean value of the completed sequence. In [21], Gregorio *et al.* propose a background initialization approach by modeling video background as ever-changing states of weightless neural networks. The background estimation of each pixel is produced by weightless neural networks designed to learn pixel color frequency. In [22], convolutional neural network (CNN) is employed to generate background patches from video sequence. A contractive stage with convolutional layers is performed to extract high-level image features. Then the refinement stage performs the deconvolution operation to transform the feature map to the final background patch. In [23], Wang *et al.* present a joint Gaussian conditional random field (JGCRF) background initialization algorithm. The target is to find optimal weights for frame fusion and it is solved as an optimization process with maximum a posteriori problem. In [24], the background extraction is modeled as a matrix decomposition problem. The spatial and temporal sparse subspace clustering is incorporated into robust principal component analysis (RPCA). The low-rank component is then taken as the estimated background. These recently proposed algorithms

improve the background performance in complex scenes, however the computational complexity also increases. Thus a robust background initialization algorithm with low complexity is still needed.

3. Proposed Background Initialization Algorithm

Since background initialization process may be heavily affected by some challenges such as illumination changes, foreground cluttering, intermittent movement and so on, a robust algorithm is needed. In this section the proposed background initialization algorithm with low complexity is introduced comprising four steps.

3.1. Overview of the Proposed Approach

As the background initialization is to eliminate moving objects, motion detection method is commonly used [13, 16, 23, 24, 25]. One simple approach is the temporal difference method in which the value differences of pixels between two consecutive frames are used to detect moving regions. This method is simple to implement but it does not consider image texture so it may leave holes in the center of a foreground object when it has uniform texture. Some other works [24, 25] compute dense optical flow to get motion information but the computational complexity is high. In this paper, to effectively detect motion regions with low complexity, the temporal difference method is combined with image superpixel segmentation called superpixel motion detection (SPMD). This approach considers both image spatial and temporal correlations to improve the background initialization performance.

The proposed algorithm comprises the following four steps, which are shown in Fig. 2.

1. The input sequence is denoted as $\mathcal{F} = \{\mathbf{F}_t\}_{t=1...T}$, where T is the length of the sequence and $\mathbf{F}_t$ stands for each frame. To cope with the gradual or sudden illumination changes in sequence, the illumination change detection by comparing the Hellinger distance of equalized histograms is performed. The longest subsequence with stable illumination condition is selected denoted as $\mathcal{S} = \{\mathbf{S}_n\}_{n=1...N, N \leq T}$.

2. For each frame, the SLIC superpixel segmentation and frame difference motion detection are performed called SPMD to generate motion mask $\mathbf{M}_n$, where n is the frame index. The superpixel with motion pixels in it is classified as foreground and is removed. After SPMD, the selected motionless pixels at position p are represented as $\mathcal{I}^p = \{i_u^p\}_{u=1...U^p}$, where U^p is the number of motionless pixels and $U^p \leq N, \forall p$.

3. Motionless pixels $\mathcal{I}^p$ are then clustered using a density-based clustering algorithm. Median value of each cluster is calculated as the reliable background candidates $\mathcal{C}^p = \{c_v^p\}_{v=1...V^p}$, where V^p is the number of cluster at position p, and V^p is typically a small number.

4. The final stationary background $\mathbf{B}$ is generated from candidates $\mathcal{C}^p$ considering both pixel number in each cluster and distance to the corresponding pixel in the first and last frame.

The proposed algorithm can generate stationary backgrounds for different scenes robustly. These four steps will be introduced in detail in the following sections.
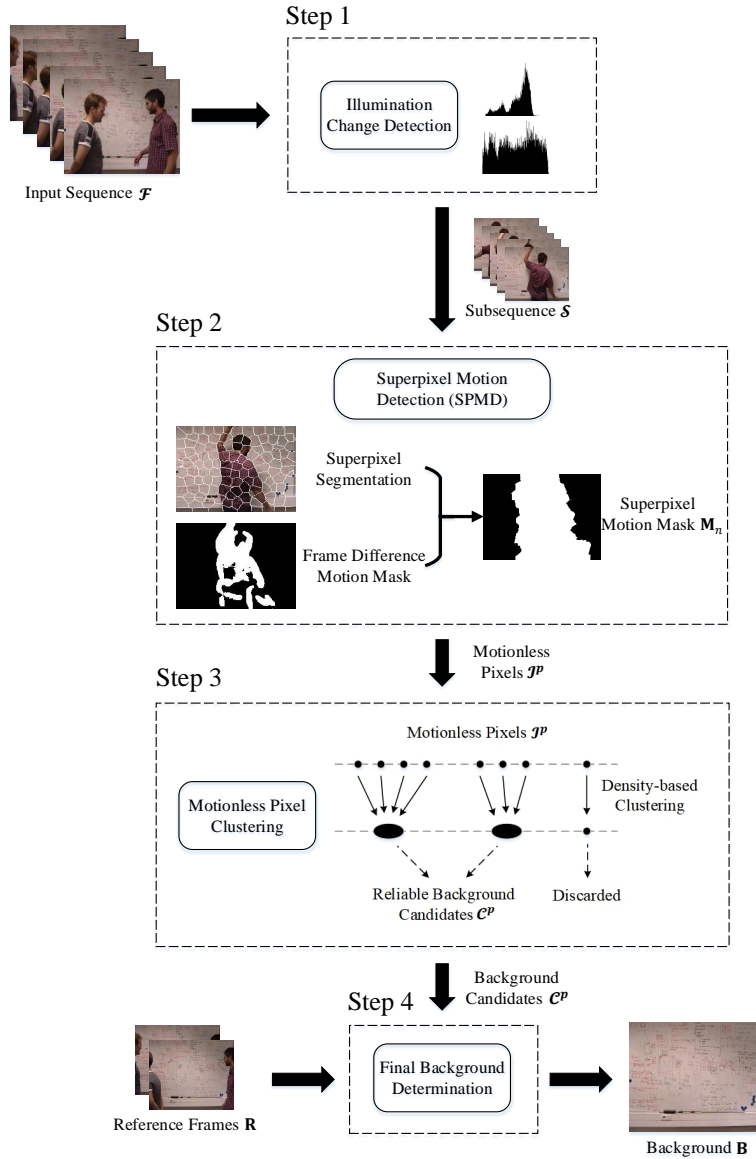
5

Fig. 2: Overview of the proposed background initialization algorithm.

3.2. Illumination Change Detection

Illumination change is common in video surveillance due to light switching, sunlight altering and so on. The main challenge when encountering illumination change is that light portion and dark portion may both exist in the result and a smudged background is produced. Thus the illumination change detection is significative and it can
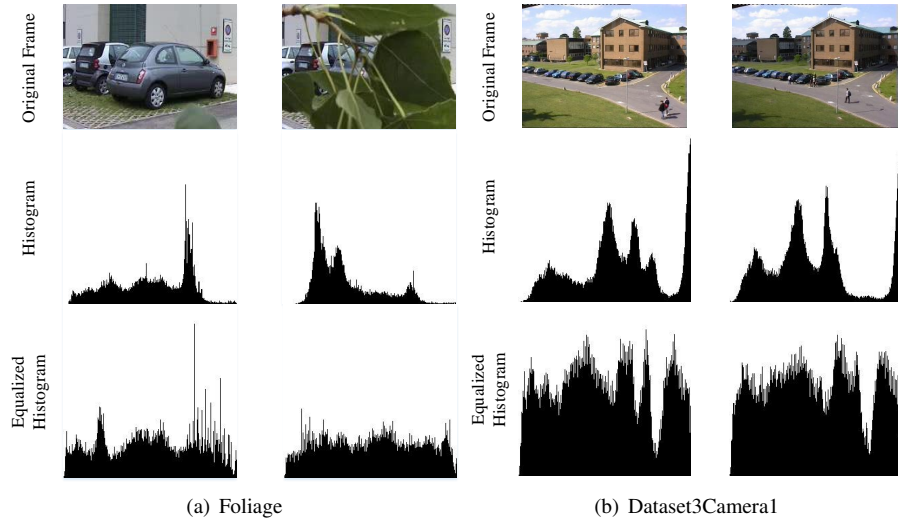
Fig. 3: Differences of histogram and equalized histogram caused by object movement and illumination change.

be included in other scene change detection applications.

In this section we mainly discuss global illumination changes. The problem is to distinguish illumination change from pixel intensity change caused by object movement. HSV color space is utilized because it is more stable than RGB space when considering illumination condition. HSV space divides the color into three components: hue (H), saturation (S) and value (V) and the value component is related to illumination strength. Therefore we employ the histogram and equalized histogram of V component to analyze the difference.

Fig. 3 shows the histogram and equalized histogram of two sequences *Foliage* and *Dataset3Camera1*. First row is the original frame, second row is histogram of V value and third row is the equalized histogram. In *Foliage*, there is no evident illumination change and the difference of two histogram is caused by movement of leaves. The shapes of two histograms are very different and even for equalized histogram, the difference is obvious. For *Dataset3Camera1*, the pixel intensity variance in two frames is mainly caused by illumination change. The shapes of two histograms are quite similar only the position of peaks are different. We can observe that when two histograms are equalized, the difference between them are significantly reduced. Based on former analysis, if the pixel intensity change is mainly caused by illumination change, the difference of value component histograms is obvious, but the equalized histograms are similar.

In the proposed illumination change detection, for a given sequence $\mathcal{F}$, the first frame is set as the initial reference frame. The histogram and equalized histogram of current frame are compared with the reference frame using Hellinger distance d_h. d_h

is calculated as:

$$d_h = \sqrt{1 - bc(H_1, H_2)}$$

$$bc(H_1, H_2) = \frac{\sum_i \sqrt{H_1(i) \cdot H_2(i)}}{\sqrt{\sum_i H_1(i) \cdot \sum_i H_2(i)}} \tag{1}$$

H_1 and H_2 stand for two histograms and i is the histogram bin index. $bc(H_1, H_2)$ is called Bhattacharyya coefficient of two histograms. Small d_h value means two histograms are similar. We denote $d_h(H)$ and $d_h(EH)$ as the Hellinger distance of two histograms and two equalized histograms, respectively. If there exists illumination change, then following condition should be satisfied:

$$\begin{cases} d_h(H) > \tau_h \\ d_h(EH) < \tau_{eh} \end{cases} \tag{2}$$

τ_h and τ_{eh} are two thresholds controlling illumination detection. If τ_h is too small, the detection is sensitive and the result may be highly affected by noises. If τ_{eh} is too large, then object movements may be wrongly classified. If illumination change is detected, a new subsequence begins and the reference frame is updated by current frame. After all frames are tested, the longest subsequence is selected denoted as $\mathcal{S}$ for further processing.

3.3. Superpixel Motion Detection (SPMD)

In SPMD, each frame in $\mathcal{S}$ is segmented using superpixel algorithm. SLIC algorithm [11] is selected because of its low computational complexity and high memory efficiency. SLIC algorithm employs the adaptive k-means clustering to group pixels in CIELAB color space. The clustering procedure begins with the initial clustering centers $[l_i, a_i, b_i, x_i, y_i]^T$ with size $L \times L$ in a regular grid. The first three components are color intensity and the last two components stand for pixel position. L is the expected approximate superpixel size. Then each pixel is assigned to the nearest cluster center with limited searching space to reduce complexity. After the assignment step, the cluster centers are updated to be the mean value of all pixels belonging to the cluster. The assignment step and update step are repeated until convergence.

Since SLIC considers a pixel as a 5-dimensional data $[l_i, a_i, b_i, x_i, y_i]^T$ with both color intensity components and spatial components. The distance measure d_{sp} is altered accordingly and is calculated as

$$d_c = \sqrt{(l_j - l_i)^2 + (a_j - a_i)^2 + (b_j - b_i)^2}$$

$$d_s = \sqrt{(x_j - x_i)^2 + (y_j - y_i)^2} \tag{3}$$

$$d_{sp} = \sqrt{d_c^2 + \left(\frac{d_s}{L}\right)^2 \cdot m^2}$$

where d_c and d_s are measurements of color proximity and spatial proximity, respectively. L is the approximate superpixel size and m is a constant. L and m are adopted

Board

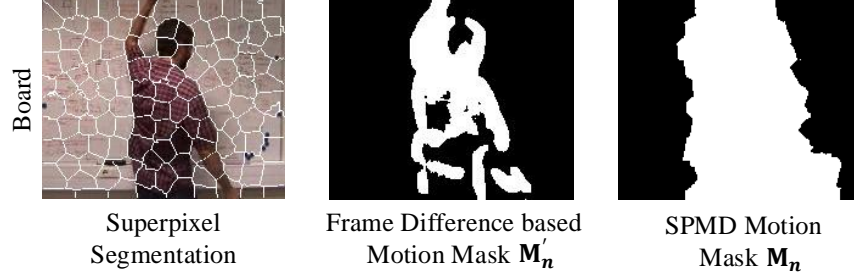| Superpixel Segmentation | Frame Difference based Motion Mask $\mathbf{M}_n'$ | SPMD Motion Mask $\mathbf{M}_n$ |

Fig. 4: Improvements in motion objects elimination of SPMD.

to normalize color proximity and spatial proximity.

In the proposed algorithm, the superpixel size L is assigned to be adaptive to image size which is calculated as

$$L = \left\lfloor \frac{min(W, H)}{\sigma_n} \right\rfloor \tag{4}$$

where W and H are width and height of the image, respectively. σ_n is the parameter controlling superpixel size.

Besides the superpixel segmentation, for a given frame $\mathbf{S}_n$ in $\mathcal{S}$, temporal frame difference is calculated as

$$\mathbf{D}_n' = |\mathbf{S}_n - \mathbf{S}_{n-1}|, n \geq 2 \tag{5}$$

In our approach, $\mathbf{S}_n$ and $\mathbf{S}_{n-1}$ are converted to the gray scale in advance so $\mathbf{D}_n'$ is a gray image as well. To avoid some noisy pixels, Gaussian filtering is performed for each pixel to get the stable temporal difference $\mathbf{D}_n$. We use Otsu method [26] to automatically calculate the frame difference based motion mask $\mathbf{M}_n'$ based on $\mathbf{D}_n$. The Otsu method calculates the optimal decision threshold τ_{opt} which minimize the intra-class variance, represented as

$$\tau_{opt} = \arg \min_g (\omega_0(g)\sigma_0^2(g) + \omega_1(g)\sigma_1^2(g)) \tag{6}$$

$\omega_0(g)$ and $\omega_1(g)$ are the probabilities of the moving and motionless pixels when the decision threshold is g. $\sigma_0^2(g)$ and $\sigma_1^2(g)$ are corresponding intra-class variance. Then the frame difference based motion mask $\mathbf{M}_n'$ can be obtained by

$$m_n'(x, y) = \begin{cases} 1, & d_n(x, y) \geq \tau_{opt} \\ 0, & d_n(x, y) < \tau_{opt} \end{cases} \tag{7}$$

where $m_n'(x, y)$ and $d_n(x, y)$ are entries of $\mathbf{M}_n'$ and $\mathbf{D}_n$ at position (x, y), respectively. Then the final SPMD motion mask $\mathbf{M}_n$ is determined combining both superpixel segmentation and $\mathbf{M}_n'$. For each superpixel region SR_i, as long as there exist moving pixels in it, the entire region SR_i is classified as a moving patch. The calculation of

$\mathbf{M}_n$ can be represented as

$$\forall (x,y) \in SR_i :$$
$$m_n(x,y) = \begin{cases} 1, & \exists(x',y') \in SR_i : m'_n(x',y') = 1 \\ 0, & otherwise \end{cases} \tag{8}$$

Fig. 4 shows an example of SPMD. For frame difference based motion detection, the corresponding motion mask $\mathbf{M}'_n$ leaves many holes in the center of foreground person because of the uniform texture. By grouping neighboring pixels in the same object using SLIC, these holes can be correctly classified as a motion patch. As a result, the unexpected errors caused by stationary moving objects or objects clustering are reduced.

3.4. Motionless Pixel Clustering

After SPMD, motion patches are eliminated and remaining motionless pixels are denoted as $\mathcal{I}^p = \{i_u^p\}_{u=1...U^p}$. p stands for pixel position and U^p is the number of pixels without motion at position p. A clustering stage is necessary to generate representative pixel intensity as reliable background candidates $\mathcal{C}^p$ for each position. Density-based clustering [27] is a simple yet efficient clustering algorithm. Different from other algorithms like k-mean clustering or mixture-of-Gaussian (MOG), it requires little knowledge of the input data and does not need to set optimal number of clusters in advance. In the proposed algorithm, the density-based clustering is employed to generate background candidates. The pixel intensity is firstly converted to the gray scale, thus the clustering process copes with scalar data.

The algorithm relies on a density-based notion of clusters. Four corresponding concepts defining density-based clustering need to be clarified:

1. ϵ-neighborhood of pixel i_u^p, denoted as $N_\epsilon(i_u^p)$, is a pixel set comprising all pixels with distance to i_u^p no larger than ϵ. That is, $N_\epsilon(i_u^p) = \{i_k^p \mid |i_k^p - i_u^p| \leq \epsilon\}$.
2. A pixel i_u^p is a core object if its ϵ-neighborhood contains at least $MinPts$ pixels, that is, $|N_\epsilon(i_u^p)| \geq MinPts$.
3. A point i_k^p is directly density-reachable from the core object i_u^p if i_k^p is in the the ϵ-neighborhood of i_u^p.
4. A pixel i_k^p is density-reachable from the core object i_u^p if there exist a chain in $\mathcal{I}^p$: $\{a_1, a_2, \ldots, a_n\}, a_1 = i_u^p, a_n = I_k^p$ such that a_{i+1} is directly density-reachable from a_i.

The objective of our density-based clustering is to find all pixels that are density-reachable from the same core object and group them together to generate a cluster set $\{\Gamma_v^p\}_{v=1...V^p}$ where V^p is the number of cluster at position p. The procedure of the algorithm is shown in Algorithm 1. Each pixel is classified whether to be a core object or not first. From the smallest core object i_k^p, the maximum density-reachable set is determined to form a cluster Γ_v^p. Since the motionless pixels $\mathcal{I}^p$ have been sorted based on gray intensity in advance, it is easy to find the largest core object i_m^p in $N_\epsilon(i_k^p)$ and this searching is iterated until $i_m^p = i_k^p$. Then, the cluster generation starts from a new core object. This iteration continues until all core objects are classified into a

Algorithm 1 Density-based clustering for background candidates generation

---

Input: $\mathcal{I}^p = \{i_u^p\}_{u=1\ldots U^p}$
Parameter: ϵ, $MinPts$
Output: background candidates $\mathcal{C}^p = \{c_v^p\}_{v=1\ldots V^p}$
       pixel number of each cluster $\mathcal{Q}^p = \{q_v^p\}_{v=1\ldots V^p}$

Prerequisite: $\mathcal{I}^p$ have been sorted based on gray intensity
Core set $\Omega = \varnothing$
for $u = 1, 2, \ldots, U^p$ **do**
   Get ϵ-neighborhood of i_u^p: $N_\epsilon(i_u^p)$
   Get number of pixels in $N_\epsilon(i_u^p)$: $|N_\epsilon(i_u^p)|$
   if $|N_\epsilon(i_u^p)| \geq MinPts$ **then**
     i_u^p is a core object and add i_u^p into Ω
   end if
end for
Number of clustering $V^p = 0$
while $\Omega \neq \varnothing$ **do**
   Find smallest pixel in Ω: i_k^p
   Find smallest pixel in $N_\epsilon(i_k^p)$ as the left boundary of i_k^p: i_l^p
   Find largest pixel in $N_\epsilon(i_k^p)$ as the right boundary of i_k^p: i_r^p
   Find largest pixel i_m^p in Ω, $s.t.$ $i_m^p \leq i_r^p$
   while $i_m^p \neq i_k^p$ **do**
     $i_k^p = i_m^p$
     Update i_r^p, i_m^p
   end while
   $V^p = V^p + 1$, Generate a new cluster $\Gamma_v^p = [i_l^p, i_r^p]$
   Remove all core objects in Γ_v^p from Ω
   Calculate $c_v^p = median(\Gamma_v^p)$
   Calculate q_v^p as the pixel number in cluster Γ_v
end while

---

cluster. Each core object is searched at most one time so the computational complexity is low. At last, the median filter is applied on each cluster to calculate the background candidates set $\mathcal{C}^p = \{c_v^p\}_{v=1\ldots V^p}$. The pixel number of each cluster is also recorded and denoted as $\mathcal{Q}^p = \{q_v^p\}_{v=1\ldots V^p}$ for final background determination.

3.5. Final Background Determination

    The final step is to generate background **B** from multiple candidates $\mathcal{C}^p$. To estimate an accurate background, the decision criteria considers both pixel number in each cluster $\mathcal{Q}^p$ and original frames in $\mathcal{S}$ as reference. It is based on the following assumptions:

1. SPMD already eliminates moving objects effectively, therefore, background component should be dominant in $\mathcal{C}^p$. The candidate with large q_v^p value is more likely to be the correct background.

2. Background has large likelihood to appear in the first frame $\mathbf{S}_1$ or the last frame $\mathbf{S}_N$. The mean value of $\mathbf{S}_1$ and $\mathbf{S}_N$ is adopted as a reference for decision, denoted as $\mathbf{R}$. If a candidate value c_v^p is close to $\mathbf{R}$, then it is potential to be selected. It is import to note that SPMD has removed most moving objects so even $\mathbf{R}$ includes foreground components, the final result is still reliable.

The decision is to choose candidates c_v^p with large q_v^p value and short distance with reference $\mathbf{R}$. It is represented as

$$b^p = \arg \max_{c_v^p} \left\{ \frac{q_v^p}{|c_v^p - r^p|} \right\} \tag{9}$$

where b^p and r^p are entries of estimated background $\mathbf{B}$ and reference $\mathbf{R}$, respectively.

The proposed background initialization algorithm adopts illumination change detection so it is robust when encountering gradual or sudden light changes. SPMD considers both image spatial correlations and temporal motion detection. It can remove relevant moving pixels more effectively. The density-based motionless pixel clustering and final background determination generate reliable background image $\mathbf{B}$ with low complexity. As a result, the proposed algorithm is robust and effective for different situations and can generate a clear background free of foreground objects for a wide range of video sequences. Next section will present the detailed experimental results.

4. Experimental Results

In this section, the performance of the proposed SPMD based background initialization algorithm is evaluated in detail. Both subjective and objective background performance are evaluated in Section 4.2. The results show that SPMD algorithm is comparable or superior to other state-of-the-art works generating the best results in complex scenarios. In addition, SPMD is a low-complexity algorithm. Section 4.3 demos that it is at least twice faster than state-of-the-art works in terms of the processing speed.

4.1. Experimental Setup

The experimental analysis is based on SBMnet dataset[2] [28]. The dataset includes 79 video sequences with resolution varying from 200×144 to 800×600. All sequences are grouped into 8 categories: *Basic*, *Intermittent Motion*, *Clutter*, *Jitter*, *Illumination Changes*, *Background Motion*, *Very Long* and *Very Short*. The dataset includes a wide range of video sequences and can help to evaluate the proposed algorithm objectively.

Six metrics are utilized to evaluate performance and they are briefly introduced. To simplify the discussion, the ground truth and estimated background are denoted as $\mathbf{B}_{GT}$ and $\mathbf{B}_E$, respectively.

1. Average Gray-level Error (AGE): It is the average of the absolute difference between $\mathbf{B}_{GT}$ and $\mathbf{B}_E$. Images are converted to gray scale in advance.

---

[2]www.scenebackgroundmodeling.net

2. Percentage of Error Pixels (pEPs): An error pixel (EP) is the pixel whose value difference between $\mathbf{B}_{GT}$ and $\mathbf{B}_E$ is larger than a threshold τ (τ is set to be 20 in [28]). pEPs is defined as the ratio of EPs and total pixels.

3. Percentage of Clustered Error Pixels (pCEPs): A clustered error pixel (CEP) is an error pixel whose four connected pixels are also error pixels. pCEPs is defined as the ratio of CEPs and total pixels.

4. Peak-Signal-to-Noise-Ratio (PSNR): PSNR is widely used to measure image quality. It is defined as

$$PSNR = 10 \cdot \log_{10} \left(\frac{MAX^2}{MSE} \right) \tag{10}$$

MSX is 255 and MSE is the mean squared error between $\mathbf{B}_{GT}$ and $\mathbf{B}_E$.

5. Multi-Scale Structural Similarity Index (MS-SSIM) [29]: This metric uses structural distortion (SSIM) as an estimation to compute perceptual image distortion, performing at multiple image scales.

6. Color image Quality Measure (CQM) [30]: CQM tries to measure perceptual image quality. PSNR values in YUV space are calculated and CQM is represented as

$$CQM = PSNR_Y \times R_W + \frac{PSNR_U + PSNR_V}{2} \times C_W \tag{11}$$

R_W and C_W are two biologically-inspired coefficients set to 0.9449 and 0.0551, respectively.

The objective of background initialization is to minimize AGE, pEPs, pCEPs so the background is accurate while PSNR, MS-SSIM and CQM should be maximized thus the perceptual background quality is high. Next section will show the background images estimated by our proposed SPMD method and the comparison with other state-of-the-art works.

4.2. Evaluation Results and Comparison

Fig 5 shows some examples of background initialization results of the proposed algorithm. The first column is a representative frame in original sequence, the second column is the true background image. Third column is the results estimated by TMF and the fourth column is produced by MOG2. The results of our proposed SPMD algorithm are shown in the last column. According to Fig 5, SPMD generages more clear backgrounds free of foreground objects compared with TMF and MOG2.

The first two sequences, *511* and *Blurred* belongs to *Basic* category with mild object motion and long-term visible background, so all methods initialize a clear background image with satisfied perceptual quality. However, following sequences are more challenging. In *Board*, the background in the central area is less visible than foreground. In *People & Foliage*, the whole scene area is heavily occupied by foreground objects and the background is divided into small isolated regions in each frame. TMF cannot estimate correct background and results of MOG2 are also blurred by foreground components, while SPMD successfully produces clear background images for

13

Fig. 5: Visual background initialization results of the proposed algorithm for sequences of SBMnet dataset.

these two sequences. There exists intermittent object motion in following three sequences *busStation*, *CaVignal* and *AVSS2007*. For instance, the man in *CaVignal* stands still in the left of the scene for the first 60% of sequence frames. Both TMF and MOG2 include foreground objects into the estimated backgrounds and produce inaccurate image for these three sequences. On the contrary, SPMD can remove motion objects

Table 1: Overall Results Comparison of SPMD and Top 7 Methods on SBMnet.

Method	AR	AGE	pEPs	pCEPs	MS-SSIM	PSNR	CQM
SPMD	1.83	**6.0988**	**0.0488**	**0.0154**	**0.9412**	29.8436	30.6827
MSCL [24]	1.67	**5.9547**	**0.0524**	**0.0171**	0.9410	**30.8952**	**31.7049**
LaBGen-OF [25]	2.33	6.1897	0.0566	0.0232	**0.9412**	**29.8957**	**30.7006**
BEWiS [21]	4.67	6.7094	0.0592	0.0266	0.9282	28.7728	29.6342
LaBGen [16]	5.17	6.7090	0.0631	0.0265	0.9266	28.6396	29.4668
LaBGen-P [31]	6.33	7.0738	0.0706	0.0319	0.9278	28.4660	29.3196
Photomontage [32]	6.50	7.1950	0.0686	0.0257	0.9189	28.0113	28.8719
SC_SOBS-C4 [33]	7.33	7.5183	0.0711	0.0242	0.9160	27.6533	28.5601

more effectively and it estimates an ideal background image for *busStation* and *CaVignal*. For *AVSS2007*, although SPMD does not remove all foreground objects, the result is still better than other two methods. The last sequence *CameraParameter* exist strong illumination change caused by light switching on. Because of the illumination change detection adopted in the proposed algorithm, the initialized background is clear and accurate, which shows the robustness of the proposed algorithm.

Besides subjective background image analysis, the results are quantitatively compared with other state-of-the-art works. Top 7 methods on SBMnet dataset are selected and they are listed here: MSCL [24], LaBGen-OF [25], BEWiS [21], LaBGen [16], LaBGen-P [31], Photomontage [32] and SC_SOBS-C4 [33]. The overall results comparison is shown in Table 1. AR means the average ranking across 6 metrics of the total 8 algorithms and each metric is calculated as the average of results on 79 sequences. Top performance is denoted by bold numbers. Table 1 shows that the proposed SPMD achieves the second best in AGE metric and the best in pEPs, pCEPs, MS-SSIM metrics. Comparison results presents that SPMD outperforms LaBGen-OF, which is the current second best method on SBMnet website. Our result is slightly worse than the best method MSCL but some metrics are comparable. Overall, SPMD can estimate accurate background for various sequences and the performance is comparable or superior to other state-of-the-art works.

As SBMnet comprises 8 categories with different video characteristics, it is necessary to evaluate performance of SPMD for individual category. Table 2 displays the evaluation results comparison for 8 categories. Because of space limitation, SPMD is compared with the top 3 methods, MSCL, LaBGen-OF and BEWiS. For category *Basic*, MSCL produces the best results. SPMD achieves comparable performance in pCEPs and MS-SSIM metrics. In other metrics, the performance is slightly worse than MSCL and ranks second. For complex scenes in *Intermittent Motion* and *Clutter*, the performance of SPMD is comparable with MSCL and LaBGen-OF, outperforming BEWiS. In category *Jitter*, all four algorithms produce similar results standing for best performance. Because of the adoption of illumination change detection, SPMD can estimate satisfied backgrounds similar to MSCL and the performance is superior to other methods. For *Background Motion*, SPMD has a close performance to BEWiS, which is the best in this category. Although our algorithm does not produces as good results as other three methods, the gap is very small and the performance is acceptable.

15

Table 2: Evaluation Results Comparison of 8 Video Categories.

Category	Method	AGE	pEPs	pCEPs	MS-SSIM	PSNR	CQM
Basic	SPMD	**3.8143**	0.0119	**0.0021**	0.9812	**33.9773**	**34.6012**
	MSCL	**3.4019**	**0.0112**	**0.0019**	0.9807	**35.1206**	**35.6507**
	LaBGen-OF	3.8421	**0.0118**	0.0033	0.9796	33.7714	34.3918
	BEWiS	4.0673	0.0162	0.0058	0.9770	32.2327	33.0035
Intermittent Motion	SPMD	**4.1840**	**0.0207**	**0.0088**	0.9745	**31.9703**	**32.7384**
	MSCL	**3.9743**	0.0313	0.0215	**0.9831**	**32.6916**	**33.4541**
	LaBGen-OF	4.6433	**0.0221**	**0.0120**	0.9676	30.5799	31.3920
	BEWiS	4.7798	0.0277	0.0173	0.9585	29.7747	30.6778
Clutter	SPMD	**4.6009**	0.0250	**0.0114**	0.9572	30.9205	31.9057
	MSCL	5.2695	0.0275	**0.0094**	0.9629	**31.3743**	**32.2837**
	LaBGen-OF	**4.1821**	0.0246	0.0117	0.9640	**32.6339**	**33.4654**
	BEWiS	10.6714	0.1227	0.0845	0.8610	25.4804	26.4783
Jitter	SPMD	9.8096	0.1123	**0.0397**	0.8501	24.3465	25.4892
	MSCL	**9.7403**	**0.1049**	0.0424	0.8475	**25.3035**	**26.3824**
	LaBGen-OF	9.2410	0.1064	**0.0380**	**0.8579**	**25.9053**	**26.9264**
	BEWiS	9.4156	**0.1048**	0.0402	**0.8524**	24.7408	25.8579
Illumination Changes	SPMD	**4.4752**	**0.0222**	**0.0090**	0.9835	**32.1318**	**32.9929**
	MSCL	**4.4319**	0.0341	**0.0134**	0.9856	**34.6735**	**35.3442**
	LaBGen-OF	8.2200	0.1130	0.0746	0.9654	27.8422	28.7690
	BEWiS	5.9048	**0.0312**	0.0223	0.9745	29.5427	30.3805
Background Motion	SPMD	**9.9119**	**0.1252**	0.0289	0.8587	25.5415	26.3356
	MSCL	11.2194	0.1540	0.0332	0.8448	24.4813	25.6982
	LaBGen-OF	10.0698	0.1312	0.0323	0.8550	**25.8626**	**26.6974**
	BEWiS	**9.6776**	**0.1258**	**0.0286**	**0.8644**	**26.0753**	**26.9685**
Very Long	SPMD	6.0924	0.0283	0.0055	0.9824	30.3164	31.1255
	MSCL	**3.8214**	0.0172	0.0022	0.9874	**32.2773**	**32.9941**
	LaBGen-OF	4.2856	**0.0114**	**0.0006**	0.9891	32.0746	32.8312
	BEWiS	**3.9652**	**0.0108**	**0.0006**	0.9891	**32.5325**	**33.2217**
Very Short	SPMD	5.9018	0.0446	0.0177	0.9423	29.5447	30.2731
	MSCL	5.7790	0.0387	**0.0131**	0.9363	**31.2396**	**31.8320**
	LaBGen-OF	**5.0338**	**0.0325**	**0.0135**	**0.9509**	**30.4959**	**31.1315**
	BEWiS	**5.1937**	**0.0345**	0.0136	**0.9488**	29.8036	30.4858

Table 3: Processing Speed Comparison for Sequences with Different Resolutions.

Sequence	Foliage	highway	I_CA_01	wetSnow	511
Resolution	200×144	320×240	352×288	536×320	640×480
SPMD	**22.8fps**	**5.6fps**	**5.2fps**	**2.9fps**	**1.6fps**
LaBGen-OF	3.3fps	1.6fps	1.2fps	0.8fps	0.5fps
BEWiS	4.3fps	2.5fps	2.2fps	1.1fps	0.6fps

The comparison shows that SPMD is robust and effective for a wide range of video sequences.

4.3. Processing Speed Analysis

Besides background image quality, the processing speed is also an important aspect when evaluating the performance of algorithm. LaBGen-OF, BEWiS and SPMD are

all implemented on a computer with Intel core i7-2600 processor for comparison. Five sequences with different resolutions from 200×144 to 640×480 are selected for evaluation. For a fair comparison, processing frames per second (fps) is recorded to denote execution speed. Table 3 presents the performance in terms of processing speed and it is noticed that SPMD is at least twice faster than other two algorithms. Especially for *Foliage*, the result of SPMD (22.8fps) is close to a realtime computing speed. For LaBGen-OF, dense optical flow with high computational complexity is performed to detect motion in a video sequence which affects processing speed. In BEWiS, a weightless neural model is used for each pixel with high computational and memory cost. For another state-of-the-art algorithm MSCL, it is reported in [24] that the computing speed is about 1.25fps for sequence *highway* on a computer with Inter core i7 processor. The computational complexity of MSCL is also high because it adopts dense optical flow for motion estimation and then an iterative optimization for matrix completion is performed. Overall, the proposed SPMD algorithm has relatively low computational complexity. The most time consuming period is superpixel segmentation and it can be further accelerated with a CPU or GPU based parallel implementation.

5. Conclusions

A background initialization algorithm based on superpixel motion detection (SPMD) is proposed in this paper. A subsequence with stable illumination condition is firstly selected making the result not affected by gradual or sudden illumination changes. Images are segmented into superpixels so spatial correlation is reserved. Frame difference based motion detection considering temporal relation is combined with superpixel segmentation, thus SPMD can effectively remove moving objects. Finally, the density-based clustering and the background determination criteria automatically generate a clear background image. Experimental results on SBMnet dataset show that the algorithm is robust and effective for a wide range of videos with performance comparable or superior with other existing works while the computational complexity is relatively low.

References

References

[1] D. K. Panda, S. Meher, Detection of moving objects using fuzzy color difference histogram based background subtraction, IEEE Signal Processing Letters 23 (1) (2016) 45–49. `doi:10.1109/LSP.2015.2498839`.

[2] X. Zhang, C. Zhu, S. Wang, Y. Liu, M. Ye, A bayesian approach to camouflaged moving object detection, IEEE Transactions on Circuits and Systems for Video Technology 27 (9) (2017) 2001–2013. `doi:10.1109/TCSVT.2016.2555719`.

[3] C. C. Chiu, M. Y. Ku, L. W. Liang, A robust object segmentation system using a probability-based background extraction algorithm, IEEE Transactions on

Circuits and Systems for Video Technology 20 (4) (2010) 518–528. `doi:10.1109/TCSVT.2009.2035843`.

[4] M. Paul, Efficient video coding using optimal compression plane and background modelling, IET Image Processing 6 (9) (2012) 1311–1318. `doi:10.1049/iet-ipr.2011.0626`.

[5] X. Li, Y. Abudoulikemu, Background-foreground information based bit allocation algorithm for surveillance video on high efficiency video coding (hevc), in: 2016 Visual Communications and Image Processing (VCIP), 2016, pp. 1–4. `doi:10.1109/VCIP.2016.7805562`.

[6] F. Chen, H. Li, L. Li, D. Liu, F. Wu, Block-composed background reference for high efficiency video coding, IEEE Transactions on Circuits and Systems for Video Technology 27 (12) (2017) 2639–2651. `doi:10.1109/TCSVT.2016.2593599`.

[7] X. Chen, Y. Shen, Y. H. Yang, Background estimation using graph cuts and inpainting, in: Proceedings of Graphics Interface 2010, 2010, pp. 97–103.

[8] T. Bouwmans, Traditional and recent approaches in background modeling for foreground detection: An overview, Computer Science Review 11 (2014) 31 – 66. `doi:http://dx.doi.org/10.1016/j.cosrev.2014.04.001`.

[9] Z. Zivkovic, Improved adaptive gaussian mixture model for background subtraction, in: Proceedings of the 17th International Conference on Pattern Recognition, 2004. ICPR 2004., Vol. 2, 2004, pp. 28–31 Vol.2. `doi:10.1109/ICPR.2004.1333992`.

[10] Z. Zivkovic, F. van der Heijden, Efficient adaptive density estimation per image pixel for the task of background subtraction, Pattern Recognition Letters 27 (7) (2006) 773 – 780. `doi:https://doi.org/10.1016/j.patrec.2005.11.005`.

[11] R. Achanta, A. Shaji, K. Smith, A. Lucchi, P. Fua, S. Ssstrunk, Slic superpixels compared to state-of-the-art superpixel methods, IEEE Transactions on Pattern Analysis and Machine Intelligence 34 (11) (2012) 2274–2282. `doi:10.1109/TPAMI.2012.120`.

[12] A. H. S. Lai, N. H. C. Yung, A fast and accurate scoreboard algorithm for estimating stationary backgrounds in an image sequence, in: Circuits and Systems, 1998. ISCAS '98. Proceedings of the 1998 IEEE International Symposium on, Vol. 4, 1998, pp. 241–244 vol.4. `doi:10.1109/ISCAS.1998.698804`.

[13] S. Amri, W. Barhoumi, E. Zagrouba, Unsupervised background reconstruction based on iterative median blending and spatial segmentation, in: Imaging Systems and Techniques (IST), 2010 IEEE International Conference on, IEEE, 2010, pp. 411–416.

[14] H. Wang, D. Suter, A Novel Robust Statistical Method for Background Initialization and Visual Surveillance, Berlin, Heidelberg, 2006, pp. 328–337. `doi: 10.1007/11612032_34`.

[15] C. Stauffer, W. E. L. Grimson, Adaptive background mixture models for real-time tracking, in: Computer Vision and Pattern Recognition, 1999. IEEE Computer Society Conference on., Vol. 2, IEEE, 1999, pp. 246–252.

[16] B. Laugraud, S. Pirard, M. V. Droogenbroeck, Labgen: A method based on motion detection for generating the background of a scene, Pattern Recognition Letters 96 (Supplement C) (2017) 12 – 21, scene Background Modeling and Initialization. `doi:https://doi.org/10.1016/j.patrec.2016.11.022`.

[17] Y. Liu, H. Yao, W. Gao, X. Chen, D. Zhao, Nonparametric background generation, Journal of Visual Communication and Image Representation 18 (3) (2007) 253 – 263. `doi:10.1016/j.jvcir.2007.01.003`.

[18] A. Elgammal, D. Harwood, L. Davis, Non-parametric Model for Background Subtraction, Springer Berlin Heidelberg, Berlin, Heidelberg, 2000, pp. 751–767. `doi:10.1007/3-540-45053-X_48`.

[19] R. Zhang, W. Gong, A. Yaworski, M. Greenspan, Nonparametric on-line background generation for surveillance video, in: Proceedings of the 21st International Conference on Pattern Recognition (ICPR2012), 2012, pp. 1177–1180.

[20] A. Sobral, E. hadi Zahzah, Matrix and tensor completion algorithms for background model initialization: A comparative evaluation, Pattern Recognition Letters 96 (Supplement C) (2017) 22 – 33, scene Background Modeling and Initialization. `doi:https://doi.org/10.1016/j.patrec.2016.12.019`.

[21] M. D. Gregorio, M. Giordano, Background estimation by weightless neural networks, Pattern Recognition Letters 96 (Supplement C) (2017) 55 – 65, scene Background Modeling and Initialization. `doi:https://doi.org/10.1016/j.patrec.2017.05.029`.

[22] I. Halfaoui, F. Bouzaraa, O. Urfalioglu, Cnn-based initial background estimation, in: 2016 23rd International Conference on Pattern Recognition (ICPR), 2016, pp. 101–106. `doi:10.1109/ICPR.2016.7899616`.

[23] H. C. Wang, Y. C. Lai, W. H. Cheng, C. Y. Cheng, K. L. Hua, Background extraction based on joint gaussian conditional random fields, IEEE Transactions on Circuits and Systems for Video Technology PP (99) (2017) 1–1. `doi:10.1109/TCSVT.2017.2733623`.

[24] S. Javed, A. Mahmood, T. Bouwmans, S. K. Jung, Background-foreground modeling based on spatiotemporal sparse subspace clustering, IEEE Transactions on Image Processing 26 (12) (2017) 5840–5854. `doi:10.1109/TIP.2017.2746268`.

[25] B. Laugraud, M. Van Droogenbroeck, Is a memoryless motion detection truly relevant for background generation with labgen?, in: Advanced Concepts for Intelligent Vision Systems, 2017.

[26] N. Otsu, A threshold selection method from gray-level histograms, IEEE Transactions on Systems, Man, and Cybernetics 9 (1) (1979) 62–66. `doi:10.1109/TSMC.1979.4310076`.

[27] M. Ester, H.-P. Kriegel, J. Sander, X. Xu, A density-based algorithm for discovering clusters a density-based algorithm for discovering clusters in large spatial databases with noise, in: Proceedings of the Second International Conference on Knowledge Discovery and Data Mining, AAAI Press, 1996, pp. 226–231.

[28] P. M. Jodoin, L. Maddalena, A. Petrosino, Y. Wang, Extensive benchmark and survey of modeling methods for scene background initialization, IEEE Transactions on Image Processing 26 (11) (2017) 5244–5256. `doi:10.1109/TIP.2017.2728181`.

[29] Z. Wang, E. P. Simoncelli, A. C. Bovik, Multiscale structural similarity for image quality assessment, in: Signals, Systems and Computers, 2004. Conference Record of the Thirty-Seventh Asilomar Conference on, Vol. 2, IEEE, 2003, pp. 1398–1402.

[30] Y. Yalman, I. Erturk, A new color image quality measure based on yuv transformation and psnr for human vision system, Turkish Journal of Electrical Engineering and Computer Sciences (2013) 603–612`doi:10.3906/elk-1111-11`.

[31] B. Laugraud, S. Pirard, M. V. Droogenbroeck, Labgen-p: A pixel-level stationary background generation method based on labgen, in: 2016 23rd International Conference on Pattern Recognition (ICPR), 2016, pp. 107–113. `doi:10.1109/ICPR.2016.7899617`.

[32] A. Agarwala, M. Dontcheva, M. Agrawala, S. Drucker, A. Colburn, B. Curless, D. Salesin, M. Cohen, Interactive digital photomontage, ACM Trans. Graph. 23 (3) (2004) 294–302. `doi:10.1145/1015706.1015718`.

[33] L. Maddalena, A. Petrosino, Extracting a background image by a multi-modal scene background model, in: 2016 23rd International Conference on Pattern Recognition (ICPR), 2016, pp. 143–148. `doi:10.1109/ICPR.2016.7899623`.